UNIVERSITY OF
BATH

University of Bath

Co-occurrence of Photochemical and Microbiological Transformation Processes in Open-Water Unit Process Wetlands

Carsten Prasse[1,2], Jannis Wenk[1,3], Justin T. Jasper[1],

Thomas A. Ternes[2], David L. Sedlak[1,*]

[1] ReNUWIt Engineering Research Center and Department of Civil & Environmental Engineering, University of California at Berkeley, Berkeley, California 94720, United States

[2] Department of Aquatic Chemistry, Federal Institute of Hydrology (BfG), Koblenz, Germany

[3] Department of Chemical Engineering and Water Innovation & Research Centre (WIRC), University of Bath, Claverton Down, Bath BA2 7AY, United Kingdom

* Corresponding author: sedlak@berkeley.edu

1   **Co-occurrence of Photochemical and Microbiological Transformation**

2   **Processes in Open-Water Unit Process Wetlands**

3

4   Carsten Prasse[1,2], Jannis Wenk[1,3], Justin T. Jasper[1], Thomas A. Ternes[2], David L. Sedlak[1*]

5

6   [1] ReNUWIt Engineering Research Center and Department of Civil & Environmental Engineering, University of

7   California at Berkeley, Berkeley, California 94720, United States

8   [2] Department of Aquatic Chemistry, Federal Institute of Hydrology (BfG), Koblenz, Germany

9   [3] Department of Chemical Engineering and Water Innovation & Research Centre (WIRC), University of Bath,

10   Claverton Down, Bath BA2 7AY, United Kingdom

11

12

13   *Corresponding author: sedlak@berkeley.edu

14

15

16

17

18

19

20

21 **Abstract**

22 The fate of anthropogenic trace organic contaminants in surface waters can be complex due
23 to the presence of multiple parallel and consecutive transformation processes. In this
24 study, the removal of five antiviral drugs (i.e., abacavir, acyclovir, emtricitabine, lamivudine
25 and zidovudine) via both bio- and photo-transformation processes was investigated in
26 laboratory microcosm experiments simulating an open-water unit process wetland
27 receiving municipal wastewater effluent. The relative importance of the two
28 transformation processes was strongly compound dependent. Phototransformation was
29 the main removal mechanism for abacavir, zidovudine and emtricitabine with half-lives
30 ($t_{1/2,photo}$) in wetland water of 1.6 h, 7.6 h and 25 h, respectively. In contrast, removal of
31 acyclovir and lamivudine was mainly attributable to slower microbial processes ($t_{1/2,bio}$ =
32 74 h and 120 h, respectively). Identification of transformation products via high-resolution
33 mass-spectrometry revealed that bio- and photo-transformation reactions took place at
34 different moieties of the molecules. For abacavir and zidovudine, rapid transformation was
35 attributable to the high reactivity of the cyclopropylamine and azido moiety, respectively.
36 Despite substantial differences in kinetics of different antiviral drugs, biotransformation
37 reactions mainly involved oxidation of hydroxyl groups to the corresponding carboxylic
38 acids. Phototransformation rates of parent antiviral drugs and their biotransformation
39 products were similar, indicating that prior exposure to microorganisms (e.g., in a
40 wastewater treatment plant or a vegetated wetland) would not affect the rate of
41 transformation of the part of the molecule that was susceptible to phototransformation.
42 However, phototransformation strongly affected the rates of biotransformation of the
43 hydroxyl groups, which in some cases resulted in greater persistence of abacavir and
44 acyclovir phototransformation products.

45
46
47
48
49
50
51

3

Introduction

The discharge of municipal wastewater effluents into surface waters can result in the presence of trace organic contaminants at concentrations that pose potential risks to aquatic ecosystems and drinking water resources. After their release, many trace organic contaminants are attenuated by biological and photochemical processes. Although these processes often occur simultaneously or sequentially in the environment, most studies have considered the occurrence of only one transformation process at a time.[1-4] Thus, it is difficult to predict which transformation products are formed and whether or not transformation reactions occurring at one moiety alter the kinetics of subsequent transformation reactions. Furthermore, if partial transformation of a compound enhances the reactivity of other moieties, interaction of transformation processes could result in changes in the distribution of transformation products as well as their rates of removal. For example, carbamazepine, a compound that is particularly resistant to biotransformation is slowly transformed upon exposure to sunlight via direct photolysis and reaction with $^{\bullet}$OH.[5,6] This leads to the formation hydroxylated derivatives[7] which are more easily biodegraded than the parent compound.[8]

Open water unit process wetlands have been developed as a polishing treatment step for municipal wastewater effluents.[9] These managed natural systems utilize sunlight to remove trace organic compounds and deactivate pathogens.[10-12] In addition, microorganisms in the biomat formed at the bottom of these treatment basins reduce nitrate and contribute to aerobic biodegradation of trace organic contaminants.[13,14] To assess the importance of the co-occurrence of biological and photochemical transformation reactions to reaction kinetics and product distribution, the fate of five antiviral drugs (i.e., abacavir, emtricitabine, lamivudine, zidovudine and acyclovir, see Figure 1) was studied under conditions comparable to those encountered in open-water unit process wetlands. Antiviral drugs were chosen because they are widely used for the treatment of diseases such as herpes, hepatitis and HIV, and have been detected at concentrations above 1 µg L^{-1} in municipal wastewater effluents.[15-18] No information about potential environmental effects resulting from the release of these compound into the aquatic environment is available so far. Furthermore, little is known about the effects of these compounds on

82 environmental viruses, a group of microorganisms that play a very important role in

83 aquatic ecosystems.[19]

84 By investigating transformation kinetics and transformation mechanisms under conditions

85 comparable to those encountered in open-water unit process wetlands it is possible to gain

86 insight into how simultaneously occurring bio- and photo-transformation reactions affect

87 the overall fate of antiviral drugs in sunlit surface waters. These compounds also serve as

88 models for other families of compounds that contain moieties that are susceptible to bio-

89 and phototransformation.

90
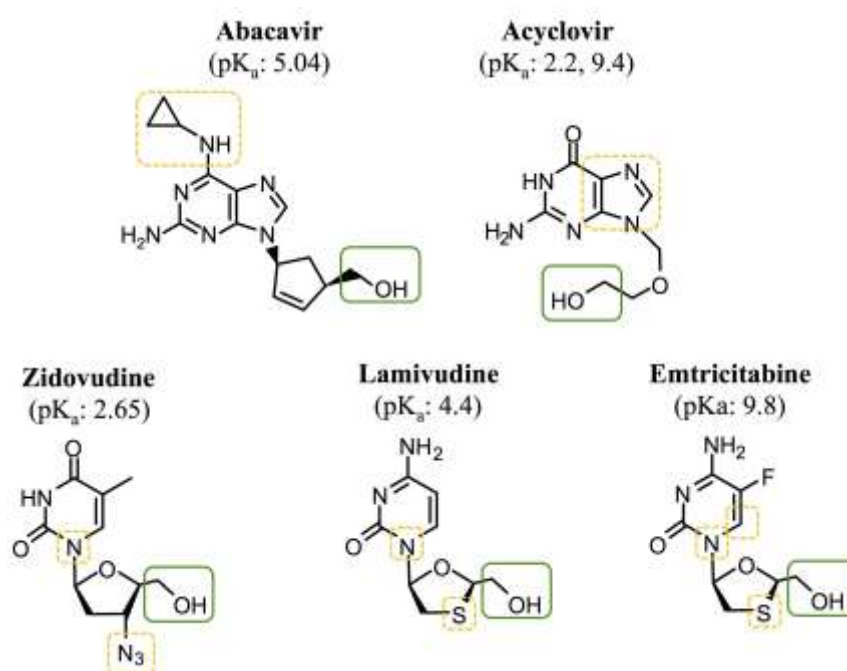
Figure 1. *Antiviral drugs and their most likely sites of proposed photo-* (⬚)
and biotransformation (▢) *reactions.*

91

Materials and Methods

Chemicals

94 Analytical reference standards of antiviral drugs and stable isotope-labeled analogues used

95 as internal standards (purity > 99%) were purchased from Toronto Research Chemicals

96 (Ontario, Canada). All other chemicals and solvents were obtained from Fisher Scientific

97 (Fairlawn, NJ).

98

Wetland water sampling conditions

Phototransformation experiments were conducted in water collected from a pilot-scale open-water unit process wetland located in Discovery Bay, CA. The facility treats about 10,000 gallons per day (4.4×10^{-4} m^3 s^{-1}) of nitrified wastewater effluent from an adjacent municipal wastewater treatment plant. Details about the open-water unit process wetland were described previously.[10,13] Water collected from the open-water wetland typically contained 10 - 20 mg L^{-1} -N NO$_3^-$, 5 - 10 mg L^{-1}-C DOC, and 60 - 80 mg L^{-1}-C dissolved inorganic carbon (HCO$_3^-$ and CO$_3^{2-}$). Samples for laboratory irradiation experiments were collected from the mid-point of the wetland. All samples were filtered through pre-rinsed 1μm (nominal pore size) glass fiber filters (Whatman) and were stored in the dark at 4°C until analysis, which occurred within 5 days.

Laboratory photo- and biotransformation experiments (or: Determination of photo- and biotransformation kinetics)

Irradiation experiments were performed using a collimated beam Oriel Solar Simulator (Spectra Physics, serial no. 91194) equipped with a 1000 W Xe lamp and either two successive atmospheric attenuation filters (Spectra Physics, serial no. 81088 & 81017) or one atmospheric and one UVB-filter (Spectra Physics, serial no. 81088 & 81050). Spectral irradiance was routinely measured with a spectroradiometer (RPS 380, International light) at different locations of the irradiated area to assess variability, which was always < 5%. Details on lamp irradiance energies and the spectra of different configurations are given in section 1.1 of the Supporting Information (SI). Irradiation experiments were carried out in 100mL black-painted glass beakers that were placed in a water bath at constant temperature (18 ± 2°C). Initial concentrations of antivirals of approximately 0.5 μM were used for all kinetics experiments. Pseudo-first order phototransformation rate constants of antivirals and photochemical probe compounds used for the quantification of reactive intermediateswere calculated from the slopes of linear regression of the natural log of concentration versus time. Control experiments in the dark revealed no degradation of antiviral drugs indicating that their transformation in wetland water can solely be attributed to photochemical processes.

129 For the elucidation of biotransformation kinetics experiments beakers were additionally
130 supplemented with 10 mL of the biomat taken from the bottom of the pilot-scale wetland
131 and kept in the dark (see Jasper et al, for further details).
132
133 *Direct and indirect phototransformation*. Experiments to assess direct phototransformation
134 of antiviral drugs were conducted in buffered ultrapure water at pH-values ranging from 6
135 to 10 (pH 6 - 8: 5 mM phosphate buffer; pH 9 - 10: 5 mM borate buffer). Samples (1 mL)
136 were collected at regular time intervals and stored at 4°C in the dark until analysis.
137 Electronic absorption spectra of antiviral drugs at different pH values (see Fig. S2) were
138 recorded with a UV-2600 UV-Vis Spectrophotometer (Shimadzu) using quartz-glass
139 cuvettes (Hellma, Germany). Further details on determination of quantum yields using the
140 *p*-nitroanisole (PNA)/pyridine(PYR) method[20] and related calculations are provided in
141 section 1.6 of the SI.
142 Indirect phototransformation of antiviral drugs was investigated by the addition of specific
143 quenchers to wetland water: *N,N*-dimethylaniline (DMA; 10 µM) was used to scavenge CO_3-
144 radicals[10], sorbic acid (2.5 mM) to scavenge excited triplet states of the dissolved organic
145 matter ($^3DOM^*$)[21], histidine (20 mM) to scavenge singlet oxygen ($^1O_2$)[22] and isopropyl
146 alcohol (IPA; 26 mM) to scavenge $^\bullet$OH-radicals.[23] In addition, experiments with specific
147 photosensitizers and were conducted in ultrapure buffered water to determine reaction
148 rate constants of antiviral drugs with individual reactive intermediates: For $CO_3^{-\bullet}$ either
149 $NaNO_3/NaHCO_3$ or $NaNO_3$/duroquinone photosensititizer methods were used.[24,25] The
150 excited triplet state photosensitizers 3-methoxyacetophenone (3MAP) and anthraquinone-
151 2-sulfonate (AQ2S) served as a proxy for $^3DOM^*$.[26] Hydroxyl-radicals were generated by
152 the irradiation of $NaNO_3$ solutions.[27] For $^1O_2$ production Rose Bengal was used as a
153 photosensitizer.[28] To further verify the role of $^1O_2$, some experiments were performed in
154 D_2O. Reaction rate constants were either determined by competition kinetics or by
155 comparing reaction rates of antiviral drugs with those of established photochemical probe
156 compounds (experimental details and calculations are provided in section 1.5 and 1.7). For
157 all indirect phototransformation experiments, the concentration changes of photochemical
158 probe compounds and antiviral drugs during irradiations were followed by HPLC-UV.
159 Experimental and analytical details, including comprehensive results are provided in SI.

160   Given the structural similarities of antivirals with DNA bases, additional irradiation
161   experiments were performed with adenine, 2-amino adenosine, cytosine, cytidine, guanine,
162   thymidine and thymine (SI section 2.1.1) to obtain further information about the
163   photoreactive moieties in the molecules and thus aid the identification of transformation
164   products.

165

166   *Identification of photo- and biotransformation products.* High resolution mass spectrometry
167   (HR-MS; LTQ Orbitrap Velos, Thermo Scientific, Bremen, Germany) was used to conduct
168   accurate MS and MS/MS analysis of transformation products of antiviral drugs. To this end,
169   experiments at elevated concentrations (40 µM) were used. The LTQ Orbitrap Velos was
170   coupled to a Thermo Scientific Accela liquid chromatography system (Accela pump and
171   autosampler). HR-MS was conducted in the positive electrospray ionization (ESI) mode. To
172   obtain structural information on the chemical structure of formed TPs, MS^n fragmentation
173   experiments were conducted using data dependent aquisition. Further information on the
174   applied setup and data dependent acquisition parameters can be found in the SI (section
175   1.2). Product formation of antiviral drugs in laboratory experiments was determined liquid
176   chromatography tandem mass spectrometry (LC/MS/MS). Details on the analytical
177   methods are provided in the SI (section 1.3).

178

179   *Combined bio- and photodegradation experiments*. The fate of antiviral drugs in the
180   presence of sunlight and microorganisms was investigated over a 72 h period in the
181   laboratory. Amber glass beakers (250mL) were filled with 180 mL of wetland water and 20
182   mL of freshly collected biomat material from the bottom of the Discovery Bay open-water
183   unit process wetland. The experimental setup was the same as described above for
184   photochemical experiments, but with three day/night cycles to simulate field conditions (8
185   h of daily irradiation followed by 16 h in the darkness; 72 h total). Antiviral drugs were
186   added individually at concentrations of 0.5 µM to ensure detection of both parent antiviral
187   compounds and their transformation products. Samples were collected at regular time
188   intervals and stored at 4°C in the dark prior to LC/MS/MS analysis, which occurred within
189   24 h. Further details about the analytical method can be found in the SI.

190

Results and Discussion

Phototransformation in wetland water

193 Phototransformation of the five investigated antiviral drugs in wetland water followed
194 first-order kinetics ($r^2 \geq 0.98$; Figure S4-S8). In native wetland water (pH 8.9), the fastest
195 phototransformation was observed for abacavir ($k_{obs} = 0.52 \pm 0.06$ h^{-1}), zidovudine ($k_{obs} =$
196 0.09 ± 0.002 h^{-1}) and emtricitabine ($k_{obs} = 0.03 \pm 0.002$ h^{-1}) whereas the transformation of
197 acyclovir and lamivudine were significantly slower ($k_{obs} = 0.012 \pm 0.001$ h^{-1} and $0.011 \pm$
198 0.001 h^{-1}, respectively) (Figure 2). No degradation of antiviral drugs in wetland water in
199 the dark was observed indicating that their removal was solely attributable to
200 photochemical processes. Photosynthetic activity leads to significant diurnal fluctuations of
201 pH in open-surface wetlands.[10] Therefore, phototransformation kinetics of antiviral drugs
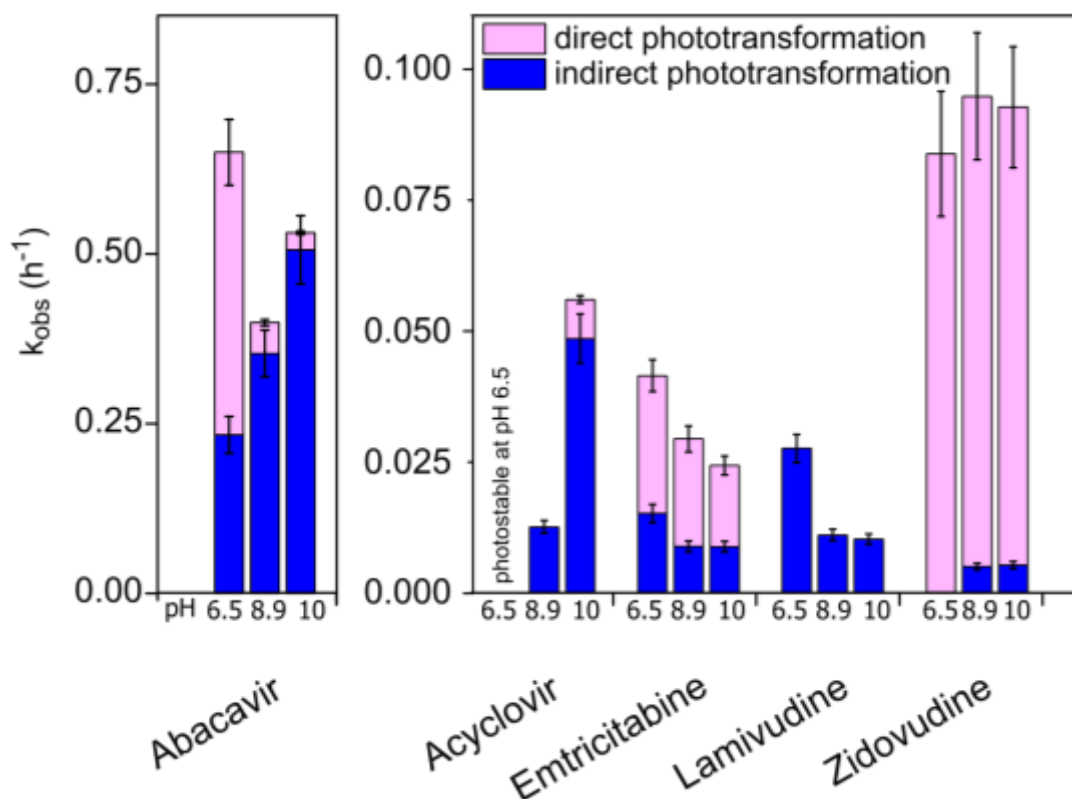202 in wetland water were also determined at pH 6.5 and pH 10 (Figure 2).

203

Figure 2. Phototransformation kinetics of antiviral drugs in experiments with wetland water at different pH values and contribution of direct and indirect photolysis processes by comparison with results obtained in ultrapure water. Data for wetland water are corrected for light-absorption. Error bars show 95% confidence intervals.

204

205 Phototransformation of abacavir in wetland water increased when the pH value was

206 adjusted to 6.5 or 10. This can be attributed to higher contribution of direct photolysis due

207 to higher quantum yields at lower pH values (i.e. Φ_{app} is 4.2 – 11.4 times higher between pH

208 6 – 8, compared to pH 9 and 10, SI Table S5) and faster indirect photolysis at higher pH

209 values. Comparison of transformation kinetics with results obtained in ultrapure water

210 revealed the dominance of indirect photodegradation processes at pH 8.9 and 10, whereas

211 direct photolysis was more important at pH 6.5. The addition of sorbic acid and histidine

212 significantly reduced phototransformation rates of abacavir in wetland water (Fig. S4),

213 suggesting the involvement of $^3DOM^*$ and $^1O_2$ in the photochemical fate of this compound.

214 This was also supported by experiments with specific singlet oxygen and excited triplet

215 state sensitizers (see below). Negligible removal of the structural analogues adenine and 2-

216 amino-adenosine further revealed that the photolability of abacavir can be attributed to the

217 cyclopropyl-moiety (see SI section 2.1.1).

218 Rates of phototransformation of zidovudine were not affected by changes in pH.

219 Comparison with reaction rates in both ultrapure water and wetland water in the presence

220 of scavengers revealed the dominance of direct photolysis (Fig. S5). Similar to abacavir,

221 comparison with the depletion of structural analogues thymine and thymidine indicated

222 that the azide moiety was responsible for the observed photoreactivity of zidovudine as

223 both analogues showed no removal when exposed to light (see SI section 2.1.1).

224 Phototransformation of acyclovir in wetland water increased with increasing pH.

225 Comparison with results from ultrapure water revealed that removal at pH 8.9 was solely

226 due to indirect photolysis, whereas at pH 10 direct photolysis was also relevant.

227 Significantly reduced rates of acyclovir phototransformation in the presence of sorbic acid

228 and histidine indicated the importance of $^1O_2$ and $^3DOM^*$ to indirect photolysis (Fig. S6). In

229 contrast to abacavir and zidovudine, phototransformation kinetics were similar to those

230 observed for the structural analogue guanine (SI Fig. S15). Thus, phototransformation of

231 acyclovir can be attributed primarily to the guanine moiety.

232 For lamivudine and emtricitabine, phototransformation kinetics in wetland water

233 decreased with increasing pH. No removal of lamivudine was observed in ultrapure water

234 indicating that its removal was entirely attributable to indirect photolysis. Higher

phototransformation rates of emtricitabine relative to lamivudine further indicated the strong influence of the fluorine atom for emtricitabine's photolability. The presence of the fluorine substituent leads to a higher absorption at 300-320 nm and thus alters the compound's UV absorbance at wavelengths between 300-320 nm (SI Fig. S2). Even though the absorption spectrum of emtricitabine did not change with pH, the quantum yield steadily decreases with increasing pH (Table S5). Phototransformation of lamivudine in wetland water was fully inhibited by sorbic acid, histidine and IPA but was unaltered in the presence of DMA (Fig. S7). This indicates the importance of $^3DOM^*$, $^1O_2$ and OH-radicals for its indirect phototransformation. For emtricitabine, phototransformation rates in wetland were only affected by IPA and sorbic acid (Fig. S8), indicating that reactions with $^1O_2$ are less important for this compound. The high photostability of its associated DNA base cytosine and nucleotide cytidine revealed the importance of structural modifications (thiol group (both compounds) and fluorine (emtricitabine)) to the observed photodegradability.

Additional experiments with individual reactive species revealed second order reaction rates with $^\bullet OH$ at or above (abacavir, zidovudine) diffusion controlled levels ranging from $5\cdot10^9 - 1.1\cdot10^{11}$ $M^{-1}s^{-1}$ (Table 1). Antiviral compounds were reactive with $CO3^{\bullet-}$, at rates between $1.2\cdot10^6 - 1.2\cdot10^9$ $M^{-1}s^{-1}$, while only abacavir ($1.2\cdot10^9$ $M^{-1}s^{-1}$) and acyclovir ($1.2\cdot10^7$ $M^{-1}s^{-1}$) were obviously reactive with $^1O_2$. With the exception of abacavir, no depletion of antiviral compounds was observe in the presence of the model triplet photosensitizer 3MAP but in presence of AQ2S at rates similar or higher than the reference probe compound TMP, indicating a selective reactivity with excited triplet states. In order to check the plausibility of results for indirect phototransformation and obtain further indications for the role of different reactive species, steady-state concentrations of reactive species measured in wetland water (Table S4) were multiplied with measured second-order reaction rate constants of antivirals with $^1O_2$, $^\bullet OH$ and $^\bullet CO_3^-$, respectively (Table 1). Based on this estimation revealed for abacavir that at pH 8.9 approximately 60% of its indirect photodegradation in wetland water can be attributed to $^1O_2$. For acyclovir the important role of $^1O_2$ for photodegradation was also strengthened, although the prediction overestimates depletion rates by a factor two. For emtricitabine and lamivudine the

265   contribution of $^1O_2$, $^\bullet OH$ and $^\bullet CO_3^-$ can be assumed negligible, emphasizing the role of $^3DOM^*$

266   and corroborating results of quenching experiments.

267

Table 1. Quantum yields (pH 9) and apparent second-order reaction rate constants of indirect phototransformation of antiviral drugs via reaction with $^1O_2$, $^\bullet OH$, $^\bullet CO_3^-$ and excited triplet states (given relative to the degradation of the $^3Sens^*$ probe compound TMP). Quantum yields of antiviral drugs at pH 6-8 and pH 10 can be found in SI Table S5.

	[M Es^{-1}]	[M^{-1} s^{-1}]				[-]	
	Φ_{app} (pH 9)	$^1O_2$	$^\bullet OH$	$^\bullet CO_3^-$ (NO$_3^-$ + HCO$_3^-$/CO$_3^{2-}$)	$^\bullet CO_3^-$ (DQ)	$^3SENS^*$ (AQ2S)	$^3SENS^*$ (MAP)
Abacavir	0.014 (±0.003)	1.2 x 10^9 (± 18%)	1.1 x 10^{11} (± 3%)	1.2 x 10^9 (± 4%)	-^{a}	4.88	13.5
Zidovudine	0.45 (±0.15)	n.d.	1.3 x 10^{10} (± 2%)	2.4 x 10^6 (± 5%)	1.3 x 10^6 (± 4%)	0.62	n.d.
Acyclovir	0.01 (±0.005)	1.2 x 10^7 (± 25%)	5.0 x 10^9 (± 2%)	1.2 x 10^8 (± 2%)	6.3 x 10^7 (± 4%)	0.08	n.d.
Emtricitabine	0.016 (±0.005)	n.d.	9.3 x 10^9 (± 2%)	3.0 x 10^6 (± 4%)	4.3 x 10^6 (± 12%)	2.03	n.d.
Lamivudine	n.d.	n.d.	9.2 x 10^9 (± 1%)	1.2 x 10^6 (± 3%)	1.7 x 10^6 (± 3%)	1.86	n.d.

268   n.d.: not detected above level of uncertainty; ^{a} not applicable due to reaction of abacavir with DQ also in the dark

269

270   *Comparison of photo- vs biotransformation rates*

271   Dark experiments conducted with wetland water in the presence of biomat material

272   indicated that biotransformation rates varied considerably among antiviral drugs.

273   Biotransformation half-life times ($t_{1/2,bio}$) ranged from 74 h for acyclovir to 500 h (21 d) for

274   emtricitabine (Fig. 3; Fig. S13). Under typical wetland treatment conditions (i.e., hydraulic

275   retention times of 2-3 days), significant biological attenuation of acyclovir and abacavir is

276   expected whereas for the other antiviral drugs removal via microbial processes is unlikely

277   to be an important removal pathway. Comparison of transformation rates of antiviral drugs

278   in the dark to those observed in irradiated wetland water indicated that

279   phototransformation processes were dominant for abacavir, zidovudine and emtricitabine,

280   while for acyclovir and lamivudine biotransformation was similar or more important than

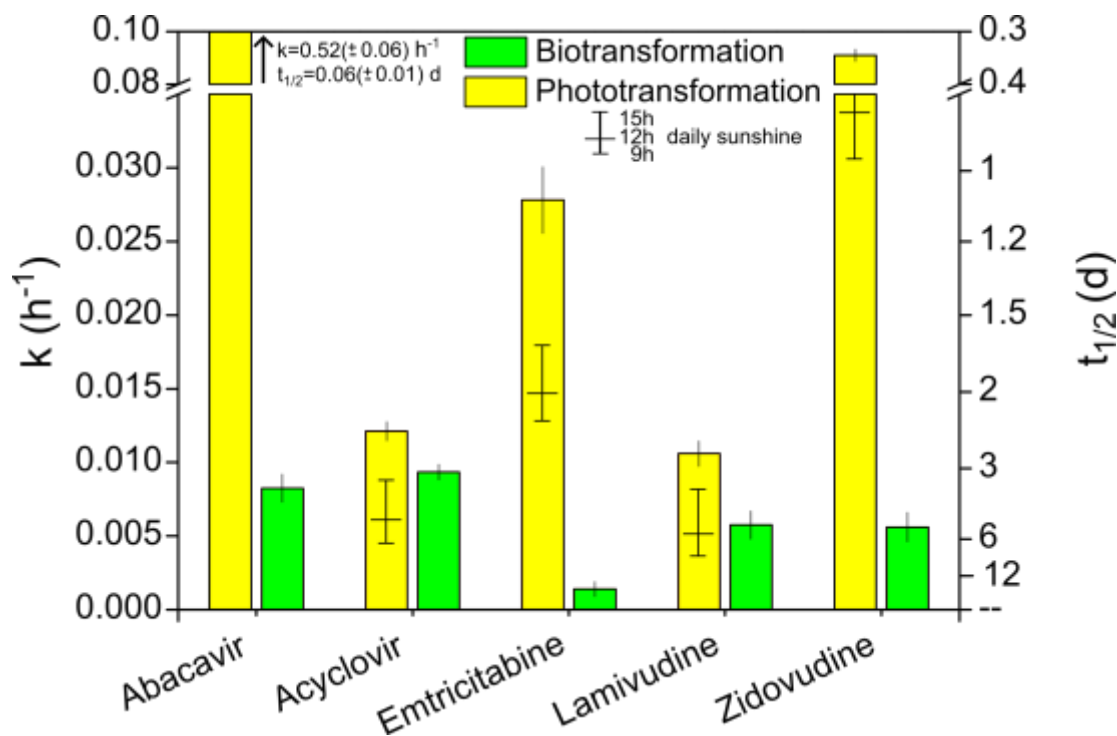281   photolysis during typical summertime conditions (Fig. 3).

282

Figure 3. Photo- and biotransformation rate constants k (h⁻¹) and associated half-life time $t_{1/2}$ (d) of antiviral drugs in laboratory experiments. Small bars within phototransformation columns indicate half-life times based on daily sunshine hours (9-15 hours). For the determination of biodegradation half-life times experiments were conducted in the presence of biomat in the dark. Error bars represent 95% confidence intervals obtained from linear regressions.

283

284 *Transformation of abacavir*

285 HRMS analysis indicated that four primary transformation products (TP318, TP288, TP284

286 and TP246) were formed during photolysis of abacavir in wetland water (SI section 2.2;

287 Table S7). In agreement with results obtained for the structural analogues 2-amino-

288 adenosine and adenine, fragmentation patterns of TP318, TP288 and TP246 revealed that

289 the cyclopropylamine moiety was the main site of reaction, leaving the 2-amino-adenine

290 (fragments: m/z 151.073, 134.046 and 109.051) and the 2-cyclopenten-1-methanyl

291 moieties (fragments: m/z 95.353 and 79.054) unaltered.

292 Exact mass calculations of TP318 showed addition of two oxygen atoms to the cyclopropyl

293 moiety (Δm +31.9898 Da). Results from MS² experiments were consistent with the scission

294 of the cyclopropyl ring and the presence of a terminal hydroxyl group, as indicated by the

295 cleavage of H_2O and CH_2O.

296 For TP288, MS data suggested modification of the cyclopropyl moiety via loss of one carbon

297 atom and the addition of one oxygen atom, leading to the formation of an acetamide,

13

298   whereas TP246 was formed via cleavage of the cyclopropyl ring. The chemical structure of

299   TP246 was confirmed by comparison with a commercially available reference standard.

300   The exact mass and fragmentation pattern of TP284 was consistent with loss of two

301   protons from either the cyclopropylamine or the 2-amino-adenosine moiety (fragments

302   m/z 149.069 and 189.088 instead of m/z 151.073 and 191.104 compared to abacavir and

303   the other TPs). Considering the high photolability of the cyclopropyl moiety, these

304   structural changes were most likely due to the formation of a cyclopropylimine.

305   To assess the relative importance of direct and different indirect photolysis processes for

306   formation of the observed abacavir transformation products, their formation was

307   investigated in buffered water (direct photolysis only), wetland water (direct and indirect

308   photolysis), and wetland water in the presence of different reactive intermediate

309   scavengers. The results revealed that both direct and indirect photolysis of abacavir

310   produced the same suite of TPs at similar relative concentrations, despite the fact that the

311   disappearance of the parent compound was significantly accelerated in the presence of

312   DOM and individual reactive intermediates (Fig. S17 & S18). Similar results were observed

313   for irgarol, an algaecide that is structurally similar to abacavir, suggesting that the

314   cycloproylamine moiety is the main site of reaction under all conditions.[29]

315   Photodegradation experiments in buffered ultrapure water with different optical filters

316   indicated that wavelengths below 320 nm preferentially led to cleavage of the cyclopropyl

317   moiety (TP246), whereas wavelengths above 320 nm (UV-A & visible light) led to scission

318   of the cyclopropyl ring followed by partial oxidation (TP318) (Fig. S19).

319   These findings suggest that phototransformation of abacavir is initiated by a one electron

320   oxidation of the cyclopropylamine moiety, leading to the formation of a

321   cyclopropylaminium radical cation,[30,31] followed by subsequent reactions resulting in the

322   formation of various products. Interestingly, this phenomenon has also been utilized for

323   the investigation of electron-hopping in DNA by modifying guanine and adenine with

324   cyclopropyl moieties.[32,33] Due to the instability of the initially formed closed ring radical

325   cation, the modification results in rapid cyclopropyl ring-opening as well as 1,2-hydrogen

326   migration, leading to the formation of an ionized allylamine.[30,34] Scission of the ring is

327   followed either by a complete cleavage of the cyclopropyl moiety (TP246) or reaction of the

328   ring opened radical cation with H_2O/O_2.[32,34] In the latter case, electron release from the

329 carbon centered radical followed by hydrolysis leads to the formation of a 3-
330 hydroxypropanaminium cation[35] and subsequent addition of water results in the formation
331 of the 3-hydroxypropanamide (TP318). In our system, TP288 is formed by photolytic
332 cleavage of the hydroxymethyl group which leads to the formation of the acetamide
333 product.[35,36] TP284 was most likely formed via H-atom abstraction, resulting in the
334 formation of a neutral cyclopropyl radical followed by an electron transfer reaction and/or
335 hydrolysis and elimination of water even though this reaction has only been shown to be
336 catalyzed by enzymes so far.[37,38]

337

338 Experiments with biomat material in the dark to determine the relative importance of
339 biotransformation reactions indicated that microbial transformation of abacavir mainly
340 occurred via oxidation of the primary alcohol group of the 2-cyclopenten-1-
341 hydroxymethanyl side chain to produce the corresponding carboxylic acid (abacavir
342 carboxylate, Fig. S13). This was consistent with previous experiments conducted with
343 mixed liquor suspended solids from an activated sludge treatment plant.[39]

344

345 When abacavir was exposed simultaneously to light and microorganisms (Fig. 4), a rapid
346 loss of abacavir was observed during the first 8-hour light period (i.e., the initial
347 concentration decreased by approximately 90 %). For the next 16 hours (i.e., the dark
348 period) abacavir removal was significantly slower. When the light was turned back on,
349 nearly all remaining abacavir disappeared. As expected, the light-induced transformation of
350 abacavir gave rise to the four photo-TPs described above (middle panel of Fig. 4). The
351 concentrations of these photo-TPs decreased by approximately 25% over the next 2.5 days,
352 indicating that further transformation took place, either via photolytic or microbial
353 processes.
354 Additional biodegradation experiments with the four photo-TPs of abacavir revealed that
355 biotransformation occurs at the same moiety as observed for the parent compound, leading
356 to the corresponding carboxylates (TP246 carboxylate, TP284 carboxylate, TP288
357 carboxylate and TP318 carboxylate; Fig. S20). Exact mass data and fragmentation patterns
358 of bio-photo TPs determined by HRMS analysis are included in section 2.2 of the SI.
359 Consequently, the observed decrease in concentration of photo-TPs shown in the middle

15

panel of Fig. 4 was mainly attributable to biotransformation, leading to a steady formation of carboxylate photo-TPs (bottom panel of Fig. 4). Faster transformation rates of abacavir photo-TPs observed during irradiation periods may have been attributable to enhanced biotransformation due to elevated oxygen concentrations or elevated pH values that occurred when the photosynthetic microorganisms in the biomat were active. Differences in biotransformation rates of TP246, TP284, TP288 and TP318, compared to abacavir (Fig. S14), indicate that alteration of chemical structure influences biotransformation kinetics, e.g. by affecting enzyme binding affinities or steric properties. Light-exposure of abacavir carboxylate formed in the dark led to its phototransformation, ultimately yielding the same photo-TPs as abacavir (bottom panel of Fig. 4). Considering that abacavir is already transformed extensively to abacavir carboxylate in activated sludge treatment,[39] a rapid elimination of both compounds can be expected in open-water unit process wetlands. In contrast to biotransformation reactions, similar phototransformation kinetics were observed for abacavir and abacavir carboxylate (Fig. S12). TP246 carboxylate was identified as the main product that accumulates over time because it is not susceptible to further reactions.
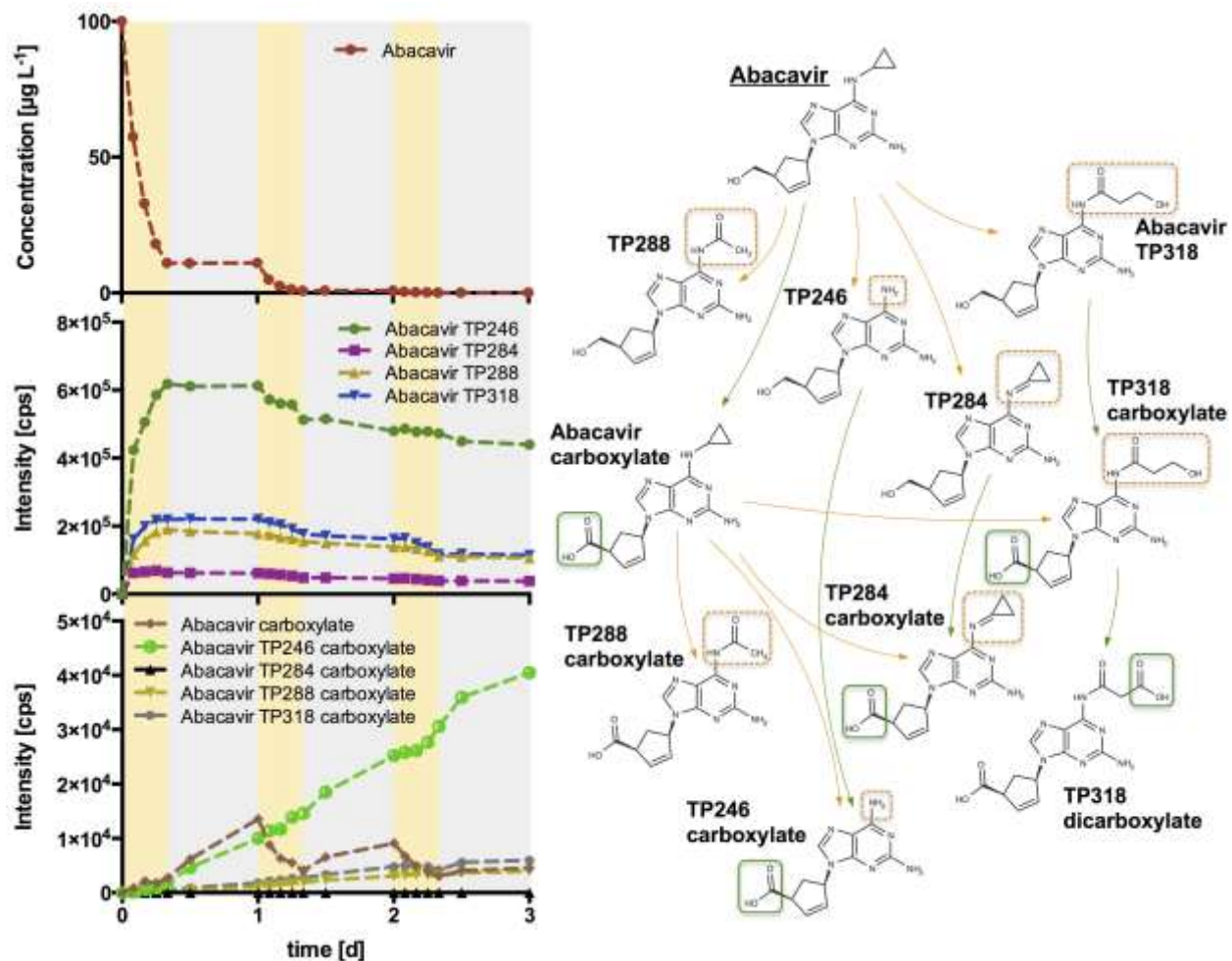
Figure 4. Transformation of abacavir (left, top) and resulting formation of photo-TPs (left, middle) and bio- / bio-photo-TPs (left, bottom)) as well as proposed transformation pathway (right) in combined in 3 day experiments in the presence of biomat with 8 hours of daily irradiation. In the transformation pathway, photo- and biotransformation reactions and structural changes in the molecules are indicated in orange and green, respectively.

376

377 *Transformation of acyclovir*

378 In contrast to abacavir, the transformation of acyclovir was dominated by microbial

379 processes (Fig. 5), with biotransformation resulting in the formation of acyclovir

380 carboxylate, which was not susceptible to further microbial transformation. These results

381 are consistent with previous biotransformation experiments conducted with acyclovir in

382 sewage sludge.[40]

383 In the absence of biomat material, exposure of wetland water to simulated sunlight

384 resulted in formation of two main photo-TPs (TP257 and TP223). HRMS analysis indicated

385 that TP257 contains two additional oxygen atoms on the guanine moiety, as evidenced by

the detection of fragment m/z 184 instead of m/z 152 (Table S8; Fig. S16). Photosensitized degradation of guanine and guanosine occurs by reaction with excited triplet states, $^1O_2$, $^{\cdot}OH$ or $^{\cdot}CO_3^-$.[41,42] The main product of the reaction of guanine with $^1O_2$ has been identified as spiroiminodihydantoin.[43-45] To assess the role of $^1O_2$ in the phototransformation of acyclovir in wetland water, experiments were conducted in both H_2O and D_2O in the presence of the $^1O_2$ sensitizer Rose Bengal (Fig. 5). Lifetimes of $^1O_2$ in D_2O are more than an order of magnitude higher than in H_2O [38] and faster transformation of acyclovir in D_2O confirmed the role of $^1O_2$ for the indirect photolysis of acyclovir. In addition, the yield of TP257 increased in D_2O. Due to its photochemical properties acyclovir is likely to undergo self-sensitation via photoexcitation and subsequent formation of $^1O_2$ as shown for guanine and guanosine.[47-49] For the second acyclovir photo-TP (TP223), HRMS analysis indicated the loss of two protons, most likely from the side chain, as evidenced by the detection of fragments m/z 152, 135 and 110, suggesting that the guanine moiety remained unchanged (Table S8). Additional information obtained from the fragmentation of the side chain was inconclusive but indicates oxidation of the terminal alcohol to the corresponding aldehyde via reaction with $^{\cdot}OH$.[50]

Results from 72h simulated sunlight experiments conducted in the presence of the biomat revealed a steady decrease of acyclovir during light and dark periods, indicating the dominance of biotransformation processes (Fig. 5b). However, biotransformation of acyclovir was significantly faster in the sunlight experiments compared to dark controls (Fig. 5a&b) suggesting that the higher oxygen concentrations and the elevated pH values that occurred when microorganisms in the biomat were undergoing photosynthesis played a role in the biotransformation processes.[10] In the presence of simulated sunlight, production of the two phototransformation products (i.e., TP257 and TP224) was observed. No significant removal of TP257 was detected during dark periods, suggesting limited biotransformation via oxidation of the terminal hydroxyl-group of the side chain. Although the exact reason for this is unknown, a plausible explanation is that the structural modifications of the guanine core moiety prevented enzymatic oxidation of TP257. In contrast, concentrations of TP223 decreased in the dark. For the biotransformation product (i.e., acyclovir carboxylate), increasing concentrations were only observed during dark periods whereas its concentration decreased when exposed to sunlight. This indicates

417   that the compound was transformed further by photolytic processes, most likely via the

418   same mechanisms as acyclovir. This was confirmed by additional irradiation experiments

419   with acyclovir carboxylate in wetland water (results not shown).
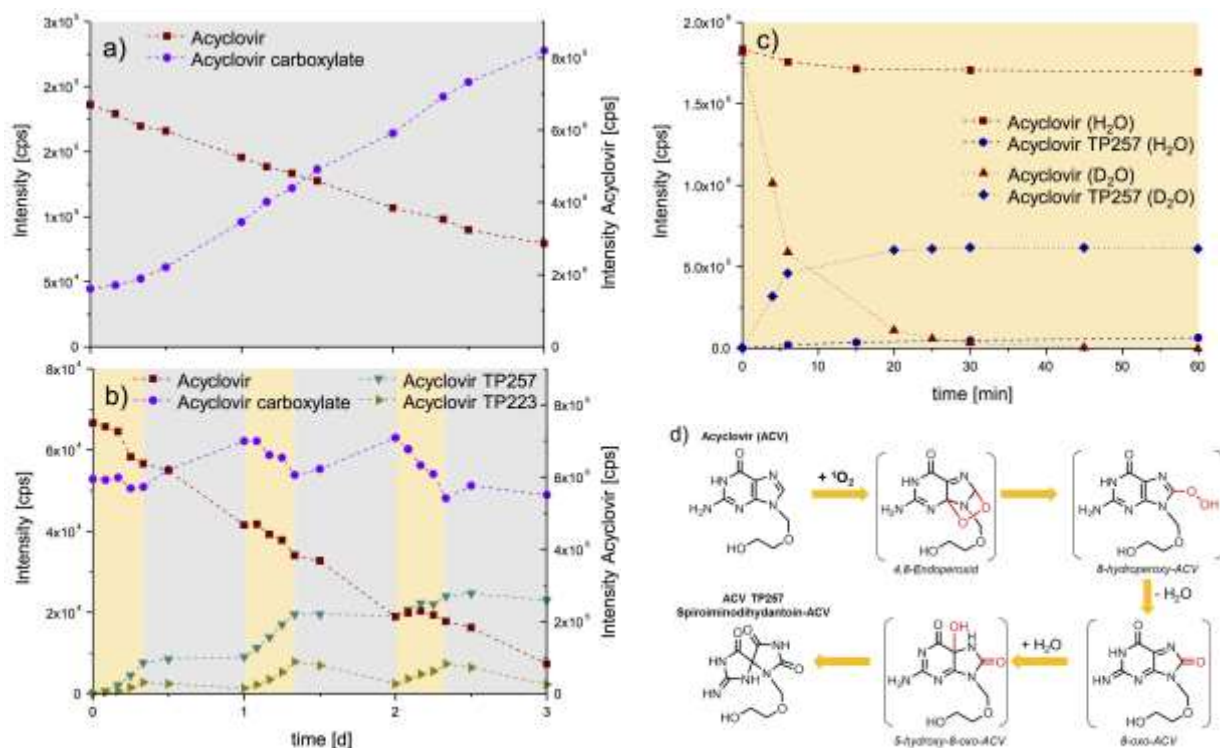
420

Figure 5. Transformation of acyclovir in the presence of biomat in the dark (a) in combined photo- and biotransformation experiments (b), as well as formation of TP257 via reaction of acyclovir with $^1O_2$ in D_2O and H_2O using Rose Bengal as photosensitizer (c) and its proposed phototransformation pathway (d). The occurrence of acyclovir carboxylate at t_0 in (a) and (b) is due to its emission by the WWTP that feeds the wetland.

421

422   *Transformation of zidovudine, lamivudine and emtricitabine*

423   MS spectra of the phototransformation products of emtricitabine, lamivudine and

424   zidovudine indicated structural changes at different positions on the molecules (Table S9-

425   S11). For lamivudine and emtricitabine, HRMS analysis revealed oxidation of the riboside

426   moiety (lamivudine TP245 and emtricitabine TP263), most likely via S-oxidation. This was

427   confirmed by comparison with commercially available reference standards. Addition of

428   H_2O to the 5-fluoro-cytosine moiety was observed for emtricitabine (emtricitabine TP265).

429   Experiments conducted with the fluorine-free analogue lamivudine illustrates the

430   importance of fluorine substitution: the F-moiety increases the light absorbance at

431 wavelengths > 300 nm (Fig. S2) for emtricitabine and leads to faster photodegradation
432 (Figure 1, Table S5). Emtricitabine TP265 was formed via hydration of the double bond of
433 the 5-fluorocytosine moiety, yielding a hydroxyl-group at position C6. For zidovudine,
434 observed phototransformations were mainly attributable to the photolability of the azido
435 moiety. Formation of zidovudine TP239 can be explained by cleavage of N_2, yielding a
436 nitrene intermediate, which reacts further via intramolecular C-H insertion to an
437 aziridine.[51,52] Subsequent nucleophilic attack of the aziridine by water leads to the
438 hydroxylation of the C atom in β-position or the formation of a hydroxylamine (zidovudine
439 TP257).[51,53] Results from HRMS analysis of zidovudine TP221 were inconclusive but
440 indicated cleavage of N_2 and H_2O from the furanosyl moiety.
441 In addition, photolytic cleavage of the nitrogen-carbon bond between the DNA base
442 moieties and the riboside analogue side chains was observed for all three compounds,
443 resulting in formation 5-fluoro-cytosine (emtricitabine TP129), cytosine (lamivudine
444 TP111) and thymine (zidovudine TP126). None of these TPs were detected in sunlight
445 experiments in the presence of biomat (Fig. S21-22), indicating that they were rapidly
446 transformed, most likely via microbial processes. For zidovudine, this was confirmed by
447 additional biodegradation experiments with the photo-TPs (i.e., thymine, TP239, TP257),
448 showing the rapid elimination of thymine (Fig. S22). Considering the importance of both
449 thymine and cytosine as DNA building blocks, it is likely that they were incorporated into
450 the microbial biomass. The fate of 5-fluorocytosine remains unclear. Similar to abacavir
451 and acyclovir, biotransformation of emtricitabine, lamivudine and zidovudine was shown
452 to result in the formation of carboxylated TPs via oxidation of the terminal alcohol as
453 already observed for abacavir and acyclovir (Fig. S13). As carboxylated TPs are expected to
454 follow the same phototransformation mechanisms as the parent compounds,, the
455 interactions of photo- and biotransformation reactions is likely to result in the complete
456 elimination of via mineralization and/or microbial uptake (Fig. 6).
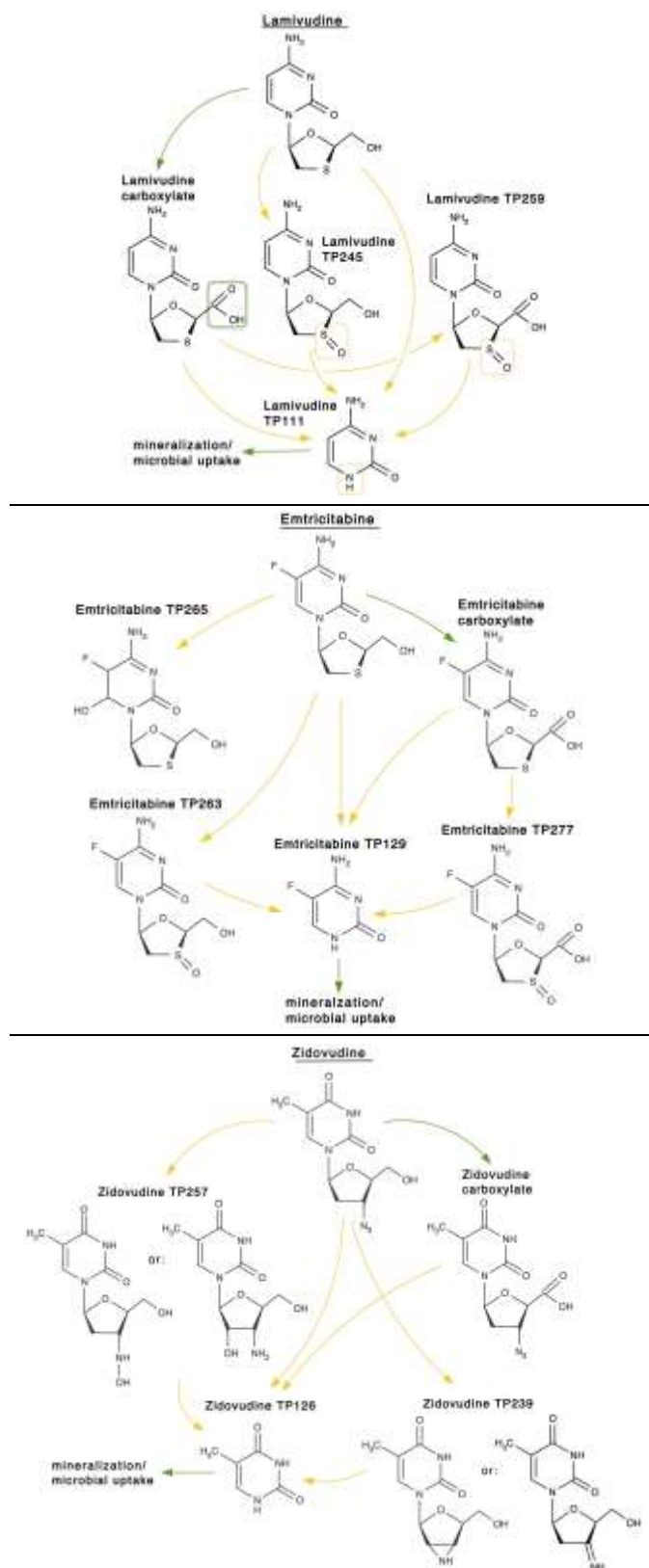457
458
459
460

Figure 6. Proposed photo- and biodegradation pathway of lamivudine (top), emtricitabine (middle) and zidovudine (bottom) in open-water wetland cells. Orange and green

461

462   *Environmental implications*

463   The differences between kinetics and transformation product formation in presence and

464   absence of the biomat highlight the complexity of transformation reactions that lead to the

465   removal of trace organic contaminants in open water unit process wetlands and other

466   sunlit waters. Attempts to predict the environmental fate of organic contaminants in these

467   systems require an understanding of both processes as well as their potential interactions.

468   Identification of TPs showed that bio- and phototransformation reactions take place at

469   different positions of the antiviral molecules. Phototransformation of biodegradation

470   products was found to occur at the same location as in the parent compound. As a result,

471   mechanisms and kinetics were similar to those observed for parent antiviral compounds.

472   This is important because carboxylate biodegradation products are typically present in

473   much higher concentrations in biological treated wastewater compared to parent

474   compounds.[32] In contrast, biodegradation kinetics of phototransformation products of

475   antiviral drugs differed substantially from that observed for the parent compound even

476   though the site of enzymatic oxidation did not change. This can be explained by differences

477   in enzyme affinities and steric hindrance. For example, phototransformation of acyclovir

478   created a transformation product (TP257) that was not susceptible to biotransformation

479   by microorganisms that could oxidize the parent compound in the dark.

480   Combining kinetic studies with investigations of transformation product formation

481   provides a better understanding of mechanisms relevant for the removal of trace organic

482   contaminants in sunlit waters. By conducting biotransformation studies in the presence

483   and absence of light it is possible to assess interactions between transformation processes

484   and the likelihood that complete mineralization of trace organic contaminants will occur.

485   These data also suggest that relative ratios of antiviral compounds and their

486   transformation products might be useful as *in situ* probes to assess the relative importance

487   of microbial and photochemical transformation pathways. This study also highlights the

488   need to consider the formation of different transformation products in sunlit and light-

489   shaded systems and the possibility of using knowledge of the reactivity of specific moieties

490 in chemical fate assessment. Considering the variety of formed transformation products,

491 there is a need for appropriate risk assessment tools to assess potential adverse effects of

492 transformation products with unknown toxicities on aquatic ecosystems. Finally, additional

493 field studies are needed to further confirm the obtained laboratory results and to assess

494 the suitability of the approach for the determination of the relative importance of

495 individual transformation processes.

496

497 **Supporting Information**

498 Additional information on sample analysis; UV spectra of antiviral drugs; determination of

499 indirect photolysis reaction rate constants, quantum yields, steady state concentrations of

500 reactive intermediates in wetland water; experiments with DNA model compounds, MS^n

501 fragments of transformation products; formation and fate of abacavir photo-TPs by

502 different reactive intermediates; results of combined bio- and phototransformation

503 experiments with emtricitabine, lamivudine and zidovudine.

504

505 **Acknowledgement**

511

512 **References**

513 (1) Burrows, H.Dl; Canle, M.; Santaballa, J.A.; Steenken, S. Reaction pathways and
514   mechanisms of photodegradation of pesticides. *J. Photoch. Photobio. B* **2002**, 67(2),
515   71-108.
516 (2) Boreen, A.L.; Arnold, W.A.; McNeill, K. Photodegradation of pharmaceuticals in the
517   aquatic environment: A review. *Aquat. Sci.* **2003**, 65(4), 320-341.
518 (3) Halling-Sorensen, B.; Nielsen, S.N.; Lanzky, P.F.; Ingerslev, F.; Lutzhoft, H.C.H.;
519   Jorgensen, S.E. Occurrence, fate and effects of pharmaceutical substances in the
520   environment - A review. *Chemosphere* **1998**, 36(2), 357-394.
521 (4) Onesios, K.M.; Yu, J.T.; Bouwer, E.J. Biodegradation and removal of pharmaceuticals
522   and personal care products in treatment systems: a review. *Biodegradation* **2009**,
523   20(4), 441-466.

(5)   Lam, M.W.; Mabury, S.A. Photodegradation of the pharmaceuticals atorvastatin, carbamazepine, levofloxacin, and sulfamethoxazole in natural waters. *Aquat. Sci.* **2005**, 67(2), 177-188.

(6)   Chiron, S.; Minero, C.; Vione, D. Photodegradation processes of the antiepileptic drug carbamazepine, relevant to estuarine waters. *Environ. Sci. Technol.* **2006**, 40(19), 5977-5983.

(7)   De Laurentiis, E.; Chiron, S.; Kouras-Hadef, S., Richard, C.; Minella, M.; Maurino, V.; Minero, C.; Vione, D. Photochemical fate of carbamazepine in surface freshwaters: Laboratory measures and modeling. *Environ. Sci. Technol.* **2012**, 46(15), 8164-8173.

(8)   Kaiser, E.; Prasse, C.; Wagner, M.; Broeder, K.; Ternes, T.A. Transformation of oxcarbazepine and human metabolites of carbamazepine and oxcarbazepine in wastewater treatment and sand filters. *Environ. Sci. Technol.* **2014**, 48(17), 10208-10216.

(9)   Jasper, J.T.; Nguyen, M.T. Jones, Z.L.; Ismail, N.S.; Sedlak, D.L., Sharp, J.O.; Luthy, R.G., Horne, A.J.; Nelson, K.L. Unit process wetlands for removal of trace organic contaminants and pathogens from municipal wastewater effluents. *Environ. Engin. Sci.* **2013**, 30(8), 421-436.

(10)   Jasper, J.T.; Sedlak, D.L. Phototransformation of wastewater-derived trace organic contaminants in open-water unit process treatment wetlands. *Environ. Sci. Technol.* **2013**, 47(19), 10781-10790.

(11)   Nguyen, M.T.; Silverman, A.I.; Nelson, K.L. Sunlight inactivation of MS2 coliphage in the absence of photosensitizers: Modeling the endogenous inactivation rate using a photoaction spectrum. *Environ. Sci. Technol.* **2014**, 48(7), 3891-3898.

(12)   Silverman, A.I.; Nguyen, M.T.; Schilling, I.E.; Wenk, J.; Nelson, K.L. Sunlight inactivation of viruses in open-water unit process treatment wetlands: Modeling endogenous and exogenous inactivation rates. *Environ. Sci. Technol.* **2015**, 49(5), 2757-2766.

(13)   Jasper, J.T.; Jones, Z.L.; Sharp, J.O.; Sedlak, D.L. Biotransformation of trace organic contaminants in open-water unit process treatment wetlands. *Environ. Sci. Technol.* **2014**, 48(9), 5136-5144.

(14)   Jasper, J.T.; Jones, Z.L.; Sharp, J.O.; Sedlak, D.L. Nitrate removal in shallow, open-water treatment wetlands. *Environ. Sci. Technol.* **2014**, 48(19), 11512-11520.

(15)   Wood, T.P.; Duvenage, C.S.J.; Rohwer, E. The occurrence of anti-retroviral compounds used for HIV treatment in South African surface water. *Environ. Pollut.* **2015**, 199, 235-243.

(16)   Peng, X.; Wang, C.; Zhang, K.; Wang, Z.F.; Huang, Q.X.; Yu, Y.Y.; Ou, W.H. Profile and behavior of antiviral drugs in aquatic environments of the Pearl River Delta, China. *Sci. Total Environ.* **2014**, 466, 755-761.

(17)   Prasse, C.; Schluesener, M.P.; Schulz, R.; Ternes, T.A. Antiviral drugs in wastewater and surface waters: A new pharmaceutical class of environmental relevance? *Environ. Sci. Technol.* **2010**, 44(5), 1728-1735.

(18)   Azuma, T.; Nakada, N.; Yamashita, N.; Tanaka, H. Synchronous dynamics of observed and predicted values of anti-influenza drugs in environmental waters during a seasonal influenza outbreak. *Environ. Sci. Technol.* **2012**, 46(23), 12873-12881.

(19)   Wommack, K.E.; Colwell. R.R. Virioplankton: Viruses in aquatic ecosystems. *Microbiol. Mol. Biol. R.* **2000**, 64(1), 69-114.

570 (20)   Dulin, D.; Mill, T. Development and evaluation of sunlight actinometers. *Environ. Sci.*
571   *Technol.* **1982**, 16(11), 815-820.

572 (21)   Grebel, J. E.; Pignatello, J. J.; Mitch, W. A. Sorbic acid as a quantitative probe for the
573   formation, scavenging and steady-state concentrations of the triplet-excited state of
574   organic compounds. *Water Res.* **2011**, 45(19), 6535–6544.

575 (22)   Boreen, A.L.; Edhlund, B.L.; Cotner, J.B.; McNeill, K. Indirectphotodegradation of
576   dissolved free amino acids: The contribution ofsinglet oxygen and the differential
577   reactivity of DOM from varioussources. *Environ. Sci. Technol.* **2008**, 42(15),
578   5492–5498.

579 (23)   Packer, J. L.; Werner, J.J.; Latch, D.E.; McNeill, K.; Arnold, W.A. Photochemical fate of
580   pharmaceuticals in the environment: Naproxen,diclofenac, clofibric acid, and
581   ibuprofen. *Aquat. Sci.* **2003**, 65(4), 342–351.

582 (24)   Vione, D.; Khanra, S.; Man, S.C.; Maddigapu, P.R.; Das, R.; Arsene, C.; Olariu, R.-I.;
583   Maurino, V.; Minero, C. Inhibition vs. enhancement of the nitrate-induced
584   phototransformation of organic substrates by the (OH)-O-center dot scavengers
585   bicarbonate and carbonate. *Water Res.* **2009**, 43(18), 4718-4728.

586 (25)   Canonica, S.; Kohn, T.; Mac, M.; Real, F.J.; Wirz, J.; Von Gunten, U. Photosensitizer
587   method to determine rate constants for the reaction of carbonate radical with
588   organic compounds. *Environ. Sci. Technol.* **2005**, 39(23), 9182-9188.

589 (26)   Bedini, A.; De Laurentiis, E.; Sur, B.; Maurino, V.; Minero, C.; Brigante, M.; Mailhot, G.;
590   Vione, D. Phototransformation of anthraquinone-2-sulphonate in aqueous solution.
591   *Photochem. Photobio. S.* **2012**, 11(9), 1445-1453.

592 (27)   Zepp, R.G.; Hoigne, J.; Bader, H. Nitrate-induced photooxidation of trace organic
593   chemicals in water. *Environ. Sci. Technol.* **1987**, 21, 443-450.

594 (28)   Burns, J.M.; Cooper, W.J.; Ferry, J.L.; King, D.W.; DiMento, B.P.; McNeill, K.; Miller, C.J.;
595   Miller, W.L.; Peake, B.M.; Rusak, S.A.; Rose, A.L.; Waite, T.D. Methods for reactive
596   oxygen species (ROS) detection in aqueous environments. *Aquat. Sci.* **2012**, 74(4),
597   683-734.

598 (29)   Sakkas, V.A.; Lambropoulou, D.A.; Albanis, T.A. Photochemical degradation study of
599   irgarol 1051 in natural waters: influence of humic and fulvic substances on the
600   reaction. *J. Photoch. Photobio. A* **2002**, 147(2), 135-141.

601 (30)   Bouchoux, G.; Alcaraz, C.; Dutuit, O.; Nguyen, M.T. Unimolecular chemistry of the
602   gaseous cyclopropylamine radical cation. *J. Am. Chem. Soc.* **1998**, 120(1), 152-160.

603 (31)   Cooksy, A.L.; King, H.F.; Richardson, W.H. Molecular orbital calculations of ring
604   opening of the isoelectronic cyclopropylcarbinyl radical, cyclopropoxy radical, and
605   cyclopropylaminium radical cation series of radical clocks. *J. Org. Chem.* **2003**,
606   68(24), 9441-9452.

607 (32)   Nakatani, K.; Dohno, C.; Saito, I. Design of a hole-trapping nucleobase: Termination
608   of DNA-mediated hole transport at N-2-cyclopropyldeoxyguanosine. *J. Am. Chem.*
609   *Soc.* **2001**, 123(39), 9681-9682.

610 (33)   Shao, F.W.; O'Neill, M.A.; Barton, J.K. Long-range oxidative damage to cytosines in
611   duplex DNA. *P. Natl. Acad. Sci. USA* **2004**, 101(52), 17914-17919.

612 (34)   Qin, X.Z.; Williams, F. Electron-spin-resonance studies on the radical cation
613   mechanism of the ring-opening of cyclopropylamines. *J. Am. Chem. Soc.* **1987**,
614   109(2), 595-597.

(35) Paul, M.M.S.; Aravind, U.K.; Pramod, G.; Saha, A.; Aravindakumar, C.T. Hydroxyl radical induced oxidation of theophylline in water: a kinetic and mechanistic study. *Org. Biomol. Chem.* **2014**, 12(30), 5611-5620.

(36) Goutailler, G.; Valette, J.C.; Guillard, C.; Paisse, O.; Faure, R. Photocatalysed degradation of cyromazine in aqueous titanium dioxide suspensions: comparison with photolysis. *J. Photoch. Photobio. A* **2001**, 141(1), 79-84.

(37) Shaffer, C.L.; Morton, M.D.; Hanzlik, R.P. N-dealkylation of an N-cyclopropylamine by horseradish peroxidase. Fate of the cyclopropyl group. *J. Am. Chem. Soc.* **2001**, 123(35), 8502-8508.

(38) Cerny, M.A.; Hanzlik, R.P. Cytochrome P450-catalyzed oxidation of N-benzyl-N-cyclopropylamine generates both cyclopropanone hydrate and 3-hydroxypropionaldehyde via hydrogen abstraction, not single electron transfer. *J. Am. Chem. Soc.* **2006**, 128(10), 3346-3354.

(39) Funke, J.; Prasse, C.; Ternes T.A. Identification and fate of transformation products of antiviral drugs formed during biological wastewater treatment (submitted).

(40) Prasse, C.; Wagner, M.; Schulz, R.; Ternes, T.A. Biotransformation of the antiviral drugs acyclovir and penciclovir in activated sludge treatment. *Environ. Sci. Technol.* **2011**, 45(7), 2761-2769.

(41) Cadet, J.; Douki, T.; Gasparutto, D.; Ravanat, J.L. Oxidative damage to DNA: formation, measurement and biochemical features. *Mutat. Res. - Fund. Mol. M.* **2003**, 531(1-2), 5-23.

(42) Neeley, W.L.; Essigmann, J.M. Mechanisms of formation, genotoxicity, and mutation of guanine oxidation products. *Chem. Res. Toxicol.* **2006**, 19(4), 491-505.

(43) Cui, L.; Ye, W.; Prestwich, E.G.; Wishnok, J.S.; Taghizadeh, K.; Dedon, P.C.; Tannenbaum S.R. Comparative analysis of four oxidized guanine lesions from reactions of DNA with peroxynitrite, singlet oxygen and y-radiation. *Chem. Res. Toxicol.* **2012**, 26(2), 195-202

(44) Luo, W.; Muller, J.G.; Rachlin, E.M.; Burrows, C.J. Characterization of spiroiminodihydantoin as a product of one-electron oxidation of 8-oxo-7,8-dihydroguanosine. *Org. Lett.* **2000**, 2(5), 613-616.

(45) Cadet, J.; Douki, T.; Ravanat, J.L. Oxidatively generated damage to the guanine moiety of DNA: Mechanistic aspects and formation in cells. *Accounts Chem. Res.* **2008**, 41(8), 1075-1083.

(46) Rodgers, M. A. J.; Snowden, P. T. Lifetime of $O_2(1\Delta g)$ in liquid water as determined by time-resolved infrared luminescence measurements. *J. Am. Chem. Soc.* **1982**, 104(20), 5541-5543.

(47) Mohammad, T.; Morrison, H. Evidence for the photosensitized formation of singlet oxygen by UVB irradiation of 2'-deoxyguanosine 5'-monophosphate. *J. Am. Chem. Soc.* **1996**, 118(5), 1221-1222.

(48) Redmond, R.W.; Gamlin, J.N. A compilation of singlet oxygen yields from biologically relevant molecules. *Photochem. Photobiol.* **1999**, 70(4), 391-475.

(49) Torun, L.; Morrison, H. Photooxidation of 2'-deoxyguanosine 5'-monophosphate in aqueous solution. *Photochem. Photobiol.* **2003**, 77(4), 370-375.

(50) von Gunten, U. Ozonation of drinking water: Part I. Oxidation kinetics and product formation. *Water Res.* **2003**, 37(7), 1443-1467.

660   (51)   Dunge, A.; Chakraborti, A.K.; Singh, S. Mechanistic explanation to the variable
661   degradation behaviour of stavudine and zidovudine under hydrolytic, oxidative and
662   photolytic conditions. *J. Pharmaceut. Biomed.* **2004**, 35(4), 965-970.
663   (52)   Gritsan, N.; Platz M. Photochemistry of azides: The azide/nitrene interface. In
664   *Organic Azides: Syntheses and Applications*; Bräse, S., Banert, K., Eds.; John Wiley &
665   Sons; 2010, pp 311-372.
666   (53)   Iwamoto, T.; Hiraku, Y.; Oikawa, S.; Mizutani, H.; Kojima, M.; Kawanishi, S. Oxidative
667   DNA damage induced by photodegradation products of 3'-azido-3'-deoxythymidine.
668   *Archives of Biochemistry and Biophysics.* 2003;416(2):155-163.
669